Indian J. pure appl. Math., **14**(5) : 646-660, May 1983

ON THE FLOW IN A RECTANGULAR CAVITY

K. D. DEBNATH

Belgharia H. S. School, Calcutta 700056

A. K. MAJUMDAR

C. M. E. R. I. Durgapur

AND

A. GHOSH

Electronics Unit, Indian Statistical Institute, 203 *Barrackpore Trunk Road, Calcutta* 700035

(*Received* 19 *December* 1981; *after revision* 31 *May* 1982)

A two-dimensional model has been assumed for flow in a rectangular cavity in an otherwise uniform surface with a turbulent free-jet boundary like flow starting from the separation point. A theoretical study of the turbulent mixing region has been made on assuming a flow variable with distance at the lower edge of this mixing region. This variable flow can be in the reverse or in the direction of the main flow depending on the depth to length ratio of the rectangular cavity and has been expressed as a series in powers of distance from the front wall. The boundary layer equations for the turbulent jet have been solved by assuming for the stream function a similar power series with variable co-efficients. The velocity profiles in the mixing region have been traced for different distributions of velocities at the lower edge of mixing region.

1. INTRODUCTION

A large number of experimental results are available for flow past rectangular cavities of different length to depth ratios due to growing interest in the heat transfer properties of such flows and in the flame stabilization in rectangular cavities. The number of theoretical works even for the cold flow problem is negligible. The main difficulty in a theoretical approach arises from the fact that the experimental results vary so much with the variation of the different parameters that it is very difficult to draw a clear picture of actual flow inside the cavity and hence to form a model for theoretical analysis. For example, Maull and East (1963), Kistler and Tan (1967), found that for values of $L/D > 0.4$ (L = length of the cavity, D = depth of the cavity) the flow inside the cavity is three-dimensional and cellular flow patterns exist and called them shallow cavities, while for $L/D < 0.4$ they found the flow to be

2-dimensional. Fox (1965a,b) could not find these features in his experiments. He concluded that this difference in experimental results might have come from the differences in the boundary layer upstream. Again, Seban (1965) in his experiments could detect 3-dimensional flow only in the forward part of all notches in the range $2 \leqslant L/D \leqslant 5$ while for $L/D = 1$, no 3-dimensional motion was detected.

Even if one neglects the 3-dimensional character of the flow, which according to Seban (1965) is confined to only the forward part of the cavity, the two dimensional flow pattern itself depends to a great extent on the length to depth ratio as is evident from the experimental results of Fox (1965a, b), Seban and Fox (1961), Haugen and Dhanak (1966, 1967). As a result it appears very difficult to develop a theory for the general case of flow over a cavity but one can take a particular range of length to depth ratio, visualise a model and then develop the theory for that case.

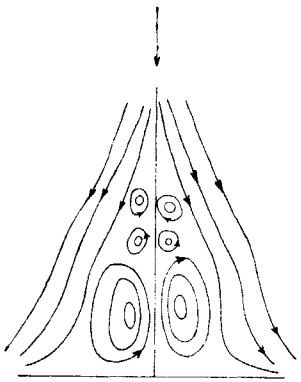

FIG. 1. Decelerating stagnation flow with separation.

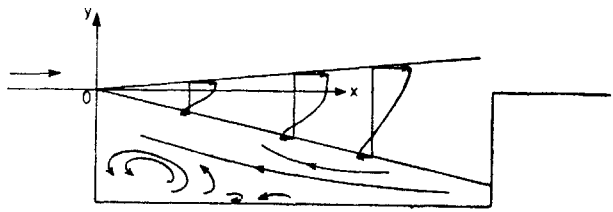

FIG. 2. Physical flow model in a shallow rectangular cavity.

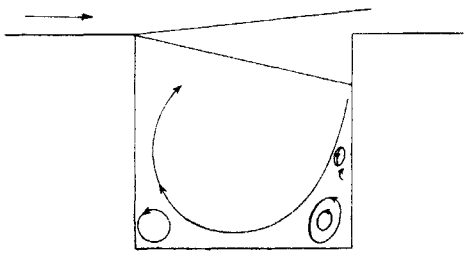

FIG. 3. Physical flow model in a square cavity.

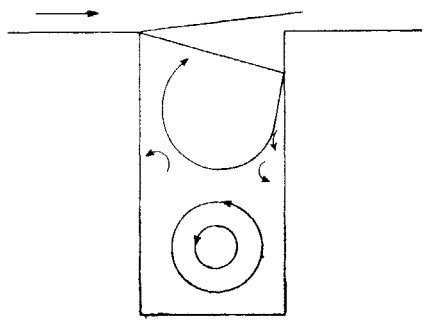

FIG. 4. Physical flow model in a deep rectangular cavity.

On examining the experimental readings available for incompressible steady flow over a rectangular cavity at high Reynolds number one can approximately describe the flow in the cavity in the following manner. The flow detaches at the upper edge of the front wall of the cavity and almost immediately there is a turbulent mixing more or less of the type of free turbulent jet. If the cavity is very shallow ($L/D>5$) this shear layer hits the bottom wall of the cavity. Charwat *et al.*(1961a, b) carried out experiments in very shallow cavities ($L/D \approx 10$) but they treated the case of supersonic flow. When the cavity is less shallow ($L/D \approx 5$) the jet after striking the backwall rebounds back immediately. This rebounded jet while approaching the lower corner of the front wall behaves like a decelerating stagnation flow with separation (Fig. 1). The stagnation point is at the lower corner of the front wall giving rise to vortices at this corner (Fig. 2). This separation has been detected in the experiments carried out by Seban (1965). When the cavity is not so shallow a part of the jet hits the backwall and turns downwards into the cavity. This turned down jet while approaching the lower corner of the backwall behaves like a decelerating stagnation flow with separation giving rise to vortices as shown in Fig. 3. If the cavity is very deep, one gets big vortices rotating alternately in opposite directions (Fig. 4). This is what has been obtained by Haugen and Dhanak (1966, 1967) in their experiments with $D/L > 1.75$. The presence of the vortices can be detected from the measurements of pressure distributions given by Haugen and Dhanak (1966, 1967) and Fox. In Seban's experiments the ratio L/D varies from 2 to 5 and in Seban and Fox (1961) it varies between 1.8 to 3.4. Their experiments in shallow cavities show that the maximum value of the rebounded flow near the bottom surface decreases linearly as it proceeds towards the front wall.

It is evident from the experimental results that the flow at the lower edge of the turbulent shear layer is not uniform. For shallow cavities the flow is in the upstream direction and if one considers the results of Seban the velocity decreases linearly as the flow approaches front wall. For deeper cavities the flow velocity at the lower edge of the shear layer is in the downstream direction and it also varies as is seen from Haugen and Dhanak's results. The magnitude and the variation of the velocity at the lower edge of the shear layer naturally depends on the length to depth ratio. Except for the case of shallow cavities the experimental readings are not sufficient to denote how the magnitude of vleocity varies along the length of the cavity. In general one can assume a power series for the variation of velocity and can choose the coefficients according to particular cases. In the present work, to analyse the turbulent shear layer, one assumes that there is steady uniform flow above it but below there is a flow varying along the length of the cavity. This variable velocity at the lower edge of the shear layer may be in the upstream direction in which case we shall call the cavity to be shallow or it may be in downstream direction when the cavity is

(Throughout the present analysis we shall call a cavity shallow when just below the turbulent shear layer the flow in the cavity is in the upstream direction. This definition is different from the one given by Kistler and Tan 1967).

deeper. The first case has been studied by Mazumdar (1972) et als assuming that the rebounded flow velocity decreases linearly as the flow proceeds towards the front wall. Here the variable velocity has been taken in the form of a power series.

2. Equations of Motion and Solution

In the theoretical analysis the flow has been assumed to be two dimensional, steady and incompressible. The origin has been taken at the upper edge of the front wall which is assumed to be the point of separation. The x-axis is parallel to the direction of the main flow and the y-axis is perpendicular to it (Fig. 2). The upstream velocity U_∞ has been taken as constant i. e., the upstream boundary layer is neglected. The flow separates from the origin and mixes with the fluid in the cavity in a turbulent free jet like flow. Instead of taking the fluid in the cavity to be at rest one assumes a velocity at the lower edge of the mixing zone as a function of x. For convenience of analysis the function has been taken as a power series in x.

Making the usual boundary layer approximation one gets the following equations for a two-dimensional turbulent mixing zone

$$u\frac{\partial u}{\partial x} + v\frac{\partial u}{\partial y} = \frac{1}{\rho}\frac{\partial \tau}{\partial y} - \frac{1}{\rho}\frac{\partial p}{\partial x} \qquad \ldots(1)$$

$$\frac{\partial u}{\partial x} + \frac{\partial v}{\partial y} = 0. \qquad \ldots(2)$$

u, v being mean velocity components of the turbulent flow and p the mean pressure.

For τ one takes the well known Prandtl formula of turbulent shearing stress

$$\tau = \rho l^2 \frac{\partial u}{\partial y}\left|\frac{\partial u}{\partial y}\right| \qquad \ldots(3)$$

$$\text{and } l = cx \qquad \ldots(4)$$

If one introduces the dimensionless velocity and lengths

$$\bar{u} = \frac{u}{U_\infty}, \bar{v} = \frac{v}{U_\infty}; \bar{x} = \frac{x}{L}, \bar{y} = \frac{y}{L}$$

(L being the length of the cavity)

the eqns. (1) and (2) reduce to

$$\bar{u}\frac{\partial \bar{u}}{\partial \bar{x}} + \bar{v}\frac{\partial \bar{u}}{\partial \bar{y}} = 2c^2\bar{x}^2\frac{\partial \bar{u}}{\partial \bar{y}}\frac{\partial^2 \bar{u}}{\partial \bar{y}^2} + \bar{U}\frac{d\bar{U}}{d\bar{x}}$$

$$\frac{\partial \bar{u}}{\partial \bar{x}} + \frac{\partial \bar{v}}{\partial \bar{y}} = 0, \qquad \ldots(5)$$

$\bar{U}$ being the dimensionless velocity outside the turbulent boundary layer. The last term in eqn. (5) will be zero for steady uniform flow.

The boundary conditions are:

$$\bar{y} \to \infty, \ \bar{u} \to 1 \qquad \ldots(6)$$

$$\bar{y} \to -\infty, \ \bar{u} \to \frac{U_1}{U_\infty} . \qquad \ldots(7)$$

U_1 being the velocity at the lower edge of the mixing region and we assume it to be of the form

$$U_1 = \frac{1}{L(2c^2)^{1/3}} \left\{ c_1\bar{x} + c_2\bar{x}^2 + c_3\bar{x}^3 + \ldots \right\} . \qquad \ldots(8)$$

With the above boundary conditions it is not possible to assume the similarity hypothesis. One assumes for the stream function the following series

$$\psi = c_0\bar{x}f_0(\eta) + c_1\bar{x}^2 f_1(\eta) + c_2\bar{x}^3 f_2(\eta) + \ldots\ldots \qquad \ldots(9)$$

where

$$\eta = \frac{\bar{y}}{\bar{x}(2c^2)^{1/3}} . \qquad \ldots(10)$$

The above ψ gives

$$\bar{u} = \frac{1}{U_\infty} \frac{\partial\psi}{L\partial\bar{y}} = \frac{1}{U_\infty L(2c^2)^{1/3}} \left\{ c_0 f_0' + c_1\bar{x} f_1' + c_2\bar{x}^2 f_2' + \ldots \right\} \qquad \ldots(11)$$

$$\bar{v} = -\frac{1}{U_\infty} \frac{\partial\psi}{L\partial\bar{x}} = \frac{1}{v_\infty L} \left\{ c_0(\eta f_0' - f_0) + c_1\bar{x}(\eta f_1' - 2f_1) + c_2\bar{x}^2(\eta f_2' - 3f_2) + \right\} . \qquad \ldots(12)$$

One takes c_0 such that

$$U_\infty = \frac{c_0}{L(2c^2)^{1/3}} . \qquad \ldots(13)$$

Substituting the above values of $\bar{u}$, $\bar{v}$ in (5) and equating the coefficients of $1/\bar{x}$, $\bar{x}$ and the free terms one gets the following sets of ordinary differential equations

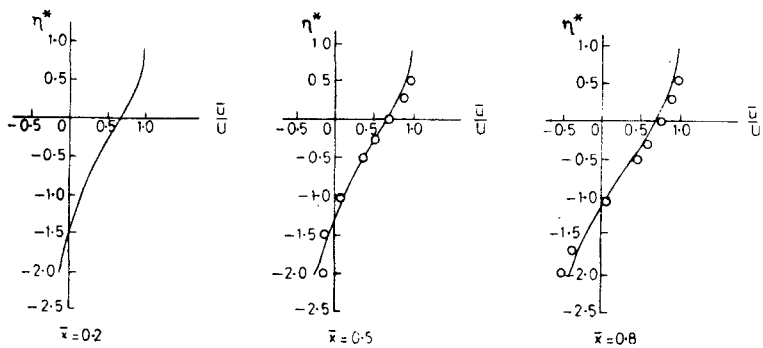

FIG. 5. Longitudinal velocity distribution at different sections of a shallow cavity.

$$f_0 + f_0''' = 0 \qquad \ldots(14)$$

$$f_0'' f_1''' - f_0' f_1' + 2 f_0'' f_1 = 0 \qquad \ldots(15)$$

$$c_0 c_2 (2 f_0' f_2' - 3 f_0'' f_2 - f_0'' f_2''') + c_1^2 (f_1'^2 - 2 f_1 f_1'' - f_1''') = 0 \qquad \ldots(16)$$

taking for $\bar{U}$ the uniform velocity outside the turbulent mixing zone and

$$c_0 c_2 (2 f_0' f_2' - 3 f_0'' f_2 - f_0'' f_2''') + c_1^2 (f_1'^2 - 2 f_1 f_1'' - f_1'' f_1''' - 1) = 0 \qquad \ldots(17)$$

for $\bar{U}$ the velocity inside the cavity i.e., $\bar{U}_1$.

It can be noted here that the term $-\frac{1}{\rho}\frac{\partial \bar{p}}{\partial \bar{x}}$ cannot contribute in the first two equations. It contributes in the equation for f_2 if one takes the velocity distribution in the cavity as the potential flow outside the turbulent mixing zone.

In order to render the functional co-efficients f_2 independent of the particular velocity distribution U_1 i.e., of c_0, c_1, c_2 etc. one splits up f_2 in the following way

$$f_2 = g_2 + \frac{c_1^2}{c_0 c_2} h_2. \qquad \ldots(18)$$

Equations (16) and (17) then give

$$2 f_0' g_2 - 3 f_0'' g_2 - f_0'' g_2''' = 0 \qquad \ldots(19)$$

and

$$2 f_0' h_2' - 3 f_0'' h_2 - f_0'' h_2''' + f_1'^2 - 2 f_1 f_1'' - f_1'' f_1''' = 0 \qquad \ldots(20)$$

(when pressure distribution is calculated assuming uniform flow outside) or

$$2 f_0' h_2' - 3 f_0'' h_2 - f_0'' h_2''' + f_1'^2 - 2 f_1 f_1'' - f_1'' f_1''' - 1 = 0 \qquad \ldots(21)$$

(when pressure distribution is calculated from the variable flow velocity inside cavity). For equation (14) one takes the boundary conditions as follows:

at the outer edge

$$\eta = \eta_1;\ \bar{u} = 1 \text{ i.e., } f_0' = 1$$

$$\frac{\partial \bar{u}}{\partial \bar{y}} = 0 \text{ i.e., } f_0'' = 0$$

$$\bar{v} = 0 \text{ i.e., } f_0 = \eta_1$$

at the inner edge i.e. at the edge inside the cavity

$$\eta = \eta_2$$

$$\bar{u} = \bar{U}_1 = \frac{c_1}{c_0}\left\{\bar{x} + \frac{c_2}{c_1}\bar{x}^2 + \ldots\right\} \text{ i.e., } f_0' = 0$$

$$\frac{\partial \bar{u}}{\partial \bar{y}} = 0 \text{ i.e., } f_0'' = 0. \qquad \ldots(22)$$

The differential equation and the boundary conditions are the same as those of Tollmien for free jet boundary and the solution is

$$f_0 = d_1 e^{-\bar{\eta}} + d_2 e^{\bar{\eta}/2} \cos\left(\frac{\sqrt{3}}{2}\bar{\eta}\right) + d_3 e^{\bar{\eta}/2} \sin\left(\frac{\sqrt{3}}{2}\bar{\eta}\right) \qquad ...(23)$$

where $\bar{\eta} = \eta - \eta_1$ and $\eta_1 = 0.981$, $\eta_2 = 2.04$, $\bar{\eta}_2 = -3.02$ ...(24)

$$d_1 = -0.0062,\ d_2 = 0.987,\ d_3 = 0.577.$$

The profile for f_0' is given in Fig. 6.

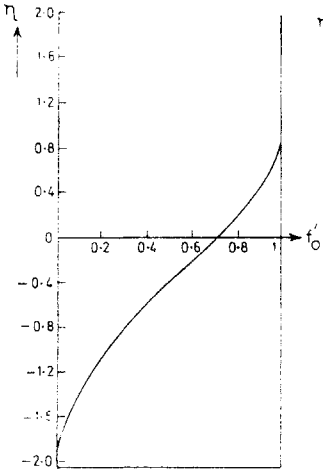

FIG. 6. The profile for f_0' against η.

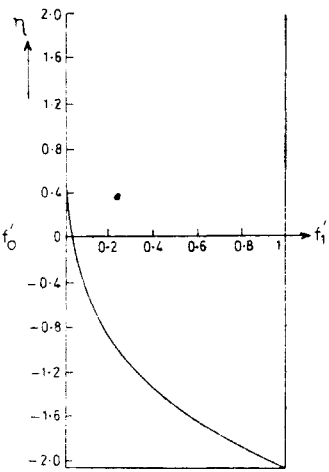

FIG. 7. The profile for f_1' against η.

To solve eqn. (15), one assumes that at the outer and lower edges η has the same values as above i.e., η_1 and η_2 respectively and to solve the third differential equation it is convenient to choose the following boundary conditions.

at the outer edge

$$\left.\begin{aligned} &\eta = \eta_1 \\ &\bar{u} = 1,\ f_0' = 1,\ \text{so, } f_1'' = 0 \\ &\frac{\partial \bar{u}}{\partial \bar{y}} = 0,\ \text{ so, } f_1'' = 0 \end{aligned}\right\}$$

at the inner edge

$$\left.\begin{aligned} &\eta = \eta_2 \\ &\bar{u} = U_1,\ f_1' = 1. \end{aligned}\right\} \qquad ...(25)$$

Equation (15) with the boundary conditions (25) could not be solved in a closed form. One can find the solution in the form of power series expansions one near $\eta = \eta_1$ and another near $\eta = \eta_2$, the two solutions being joined at an intermediate point.

Near $\eta = \eta_1$, the series is assumed in the form

$$f_1(\eta) = A_0 + A_1 X + A_2 \frac{X^2}{2!} + A_3 \frac{X^3}{3!} + \ldots \quad \ldots(26)$$

where

$$X = \eta - \eta_1. \quad \ldots(27)$$

Using boundary conditions at $\eta = \eta_1$, one gets

$$A_1 = A_2 = 0. \quad \ldots(28)$$

Near $\eta = \eta_2$, one assumes a series

$$f_1(\eta) = B_0 + B_1 Y + B_2 \frac{Y^2}{2!} + B_3 \frac{Y^3}{3!} + \ldots \quad \ldots(29)$$

where

$$Y = \eta - \eta_2 \quad \ldots(30)$$

The boundary condition at η_2 gives $B_1 = 1$. $\ldots(31)$

From the solution (23) for f_0 one can also expand f_0 in series near η_1 and η_2. They are

$$f_0(\eta) = E_0 + E_1 X + E_2 \frac{X^2}{2!} + E_3 \frac{X^3}{3!} + \ldots \quad \ldots(32)$$

where

$$\left.\begin{aligned} &E_0 = -E_3 = E_6 = -E_9 = \ldots\ldots = 0.981 \\ &E_1 = -E_4 = E_7 = -E_{10} = \ldots\ldots = 1 \\ &E_2 = E_5 = E_8 = E_{11} = \ldots\ldots = 0 \end{aligned}\right\} \quad \ldots(33)$$

and

$$f_0(\eta) = D_0 + D_1 Y + D_2 \frac{Y^2}{2!} + D_3 \frac{Y^3}{3!} + \ldots\ldots \quad \ldots(34)$$

where

$$\begin{aligned} &D_0 = -D_3 = D_6 = -D_9 = \ldots\ldots = -0.3800 \\ &D_1 = D_4 = D_7 = D_{10} = \ldots\ldots = 0 \\ &D_2 = D_5 = D_8 = D_{11} = \ldots\ldots = 0. \end{aligned} \quad \ldots(35)$$

Substituting the series (26) and (32) in equation (15) and equating co-efficients of different powers of X one gets A_3, A_4, A_5, etc. in terms of A_0. Similarly substituting the series (29) and (34) in equation (15) and equating co-efficients of different powers of Y one gets B_3, B_4, etc. in terms of B_0 and B_2. To determine these three unknown constants A_0, B_0 and B_2 one matches the values of f_1, f_1' and f_1'' obtained from the series (26) and (29) at an intermediate point $\eta = -0.24$.

The values of the constants thus obtained are

$$\left.\begin{array}{lll} A_0 = 0.03255, & B_0 = -0.72506, & B_7 = 0.3 \\ A_1 = 0, & B_1 = 1.0, & B_8 = 1.26466 \\ A_2 = 0, & B_2 = -1.26466, & B_9 = 5.80046 \\ A_3 = 0.0651, & B_3 = 1.45012, & B_{10} = -13.05 \\ A_4 = -0.03318, & B_4 = -1.5, & B_{11} = 1.26466 \\ A_5 = 0.04509, & B_5 = 1.26466, & B_{12} = 104.55365 \\ A_6 = -0.11299, & B_6 = -0.72506, & \\ A_7 = 0.08751, & & \\ A_8 = 0.08004, & & \end{array}\right\} \quad \ldots(36)$$

The profile f_1' has been traced in Fig. 7.

Next to solve equation (19) for the function g_2 one again assumes that at the outer and inner boundaries η has the same values as above viz. η_1 and η_2.

For the boundary conditions one chooses the following.

At the outer edge

$$\eta=\eta_1;\ \bar{u} \to 1,\ f_0' \to 1,\ \text{so } f_2' = 0 \text{ i.e. } g_2' = 0 \text{ and } h_2' = 0$$

$$\frac{\partial \bar{u}}{\partial \bar{y}} = 0;\ g_2'' = 0,\ h_2'' = 0.$$

At the lower edge

$$\eta = \eta_2;\ \bar{u} \to \overline{U}_1,\ f_2' \to 1,\ \text{i. e., } g_2' \to 1,\ h_2' \to 0. \qquad \ldots(37)$$

To solve eqn. (19), one adopts the same procedure as that used to solve eqn. (15). Near $\eta = \eta_1$, one assume a series for g_2 in the form

$$g_2 = F_0 + F_1 X + F_2 \frac{X^2}{2!} + F_3 \frac{X^3}{3!} + \ldots\ldots \qquad \ldots(38)$$

where

$$X = \eta - \eta_1$$

near $\eta = \eta_2$ the series assumed is

$$g_2 = P_0 + P_1 Y + P_2 \frac{Y^2}{2!} + \ldots\ldots \qquad \ldots(39)$$

where

$$Y = \eta - \eta_2.$$

Using the same procedure of matching as used for solving the equation for f_1 one gets the following values for the co-efficients of the power series.

$$
\left.\begin{array}{lll}
F_0 = -0.01595, & P_0 = -0.612179, & P_6 = 0 \\
F_1 = 0, & P_1 = 1 & P_7 = 1.4 \\
F_2 = 0, & P_2 = -1.45017, & P_8 = -1.45017 \\
F_3 = 0.04797, & P_3 = 1.83635, & P_9 = 16.52724 \\
F_4 = -0.048899, & P_4 = -2, & P_{10} = -43.1, \\
F_5 = +0.083077, & P_5 = 1.45017, & P_{11} = 1.45017 \\
F_6 = -0.161594, & & P_{12} = 396.65376. \\
F_7 = -0.218773, & & \\
F_8 = -0.2663328, & &
\end{array}\right\} \quad \ldots(40)
$$

The profile for g_2' is given in Fig. 8.

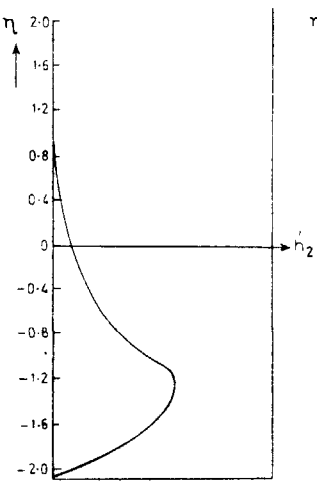

FIG. 8. The profile for h_2' against η.

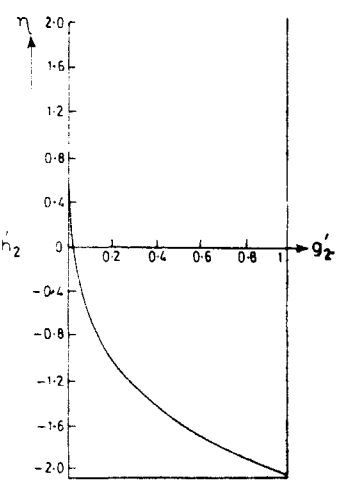

FIG. 9. The profile for g_2' against η.

To find h_2 one comes across a new difficulty. The term $\bar{U}\dfrac{d\bar{U}}{dx}$ does not contribute anything in the equations for f_0 and f_1 but it does influence the equation for f_2. As has already been noted we get two different differential equations (16) and (17) for f_2 depending on the potential flow assumed outside the turbulent mixing region. If one assumes that the pressure is to be determined from the uniform flow velocity U_∞, one gets eqn. (16). If on the otherhand one assumes that the pressure distribution in the boundary layer type mixing region is controlled by the flow in the cavity one gets eqn. (17). It is known that there is no significant variation of pressure distribution in the jet mixing region so it apparently seems that any one of the equations (16)

or (17) can be taken without involving appreciable error. But while trying to solve eqn. (20) for h_2 with the boundary conditions given in (37) it was found that the boundary condition at $\eta = \eta_2$ gave absurd results. Similarly if one takes eqn. (21) for h_2 one finds that the boundary condition at $\eta = \eta_1$ gave absurd results. This must be due to s ome inherent characteristics of the boundary layer simplifications. It was then found advantageous to choose as before for h_2 two power series one valid near $\eta = \eta_1$ and the other near $\eta = \eta_2$. The series valid near η_1 was substituted in eqn. (20) to determine the co-efficients while the series valid near η_2 was substituted in eqn. (21) to determine the co-efficients. The unknown constants were determined by the same method as for f_1 and g_2.

The series near η_1 is

$$h_2(\eta) = H_0 + H_1 X + H_2 \frac{X^2}{2!} + \ldots \qquad \ldots(41)$$

and that near η_2 is

$$h_2(\eta) = K_0 + K_1 Y + K_2 \frac{Y^2}{2!} + K_3 \frac{Y^3}{3!} + \ldots \qquad \ldots(42)$$

The values of the co-efficients obtained are

$$\left.\begin{aligned} &H_0 = -0.04005,\ H_1 = 0,\ H_2 = 0,\ H_3 = 0.12015,\ H_4 = -0.12465, \\ &H_5 = 0.21586,\ H_6 = -0.39929,\ H_7 = 0.57251, \\ &K_0 = -0.62404,\ K_1 = 0,\ K_2 = 1.59254,\ K_3 = -3.11992, \\ &K_4 = 4.01244,\ K_5 = -4.66345,\ K_6 = -0.99841,\ K_7 = 13.6377. \end{aligned}\right\} \qquad \ldots(43)$$

The profile for h_2' thus obtained is given in Fig. 9.

3. Application

(a) *Application of the Results in the Case of Shallow Cavity*

It has already been discussed in section 1 that in the case of shallow cavity ($L/D \approx 5$), the jet after striking the backwall rebounds back immediately. This rebounded jet while proceeding towards the upstream wall behaves like a decelerating stagnation flow (Fig. 2). Seban's experiments show that the rebounded flow velocity is maximum near the downstream wall and decrease more or less linearly as it proceeds towards the unstream wall of the cavity. So, for this case one assumes

$$\frac{U_1}{U_\infty} = \frac{c_1}{c_0}\bar{x} (c_1 < 0). \qquad \ldots(44)$$

The velocity components in the jet mixing region have the form

$$\left.\begin{aligned} \bar{u} &= f_0' + \frac{c_1}{c_0}\,\bar{x}\,f_1' \\ \bar{v} &= (2c^2)^{1/3}\,\{(\eta f_0' - f_0) + c_1\bar{x}(\eta f_1' - 2f_1)\}\,. \end{aligned}\right\} \quad \ldots(45)$$

From the experimental results of Seban (1965) and Seban and Fox (1961), it appears that the maximum reverse velocity is about $0.6U_\infty$. If one chooses this value then

$$\frac{c_1}{c_0} = -\,0.6 \quad \ldots(46)$$

and the velocity profiles for $\bar{u}$ at different points $\bar{x} = 0.2,\ 0.5,\ 0.8$ along the cavity are then given by Fig. 5. The transverse width of the jet increases linearly according to the formula $b = 0.255\,\bar{x}$. Experimental points of Majumdar *et al.* (1972) for the case $L/D \simeq 5$ have been shown in the figure for comparison. The agreement is quite satisfactory.

(b) *Application of the Results for the Case of Non-shallow Cavities*

As has already been mentioned it is not possible, from experimental results available to predict how the velocity at the lower edge of the shear layer varies along the length of the cavity. The form we have choosen for the velocity U_1 assumes that the magnitude of velocity is zero at the front wall. It may then increase and reach a maximum value and then diminish or may go on continuously increasing before hiting the backwall. By choosing different value for the parameters c_1/c_0 and c_2/c_0 one can get such different distribution of velocities.

We have

$$\bar{U} = \frac{c_1}{c_0}\,\bar{x} + \frac{c_2}{c_0}\,\bar{x}^2\,. \quad \ldots(47)$$

This will have a maximum value in $0 < x < 1$, if $\frac{c_2}{c_0}$ is negative and the maximum is reached at $\bar{x} = -\frac{c_1}{2c_2}$ and $(\bar{U}_1)_{\max} = -\frac{1}{4}\left(\frac{c_1^2}{c_0 c_2}\right)$.

A few particular cases have been studied and the corresponding velocity profiles at the stations $\bar{x} = 0.2,\ 0.5$ and 0.8 have been traced.

Case I: $\frac{c_1}{c_0} = 0.5,\ \frac{c_2}{c_0} = -\,0.5$.

Here $\bar{U}_1 = 0$ at $\bar{x} = 0$ and $\bar{x} = 1$, the maximum velocity is reached at $\bar{x} = 0.5$ and its value is given by $(\bar{U}_1)_{\max} = \frac{1}{8}$.

The profiles are given in Fig. 10.

Case II: $\frac{c_1}{c_0} = 0.8,\ \frac{c_2}{c_0} = -\,0.8$.

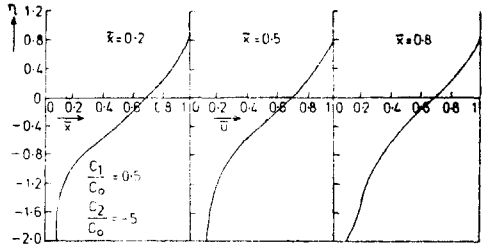

FIG. 10. Longitudinal velocity distribution in a non-shallow cavity for different values of $\frac{c_1}{c_0}$ and $\frac{c_2}{c_0}$.

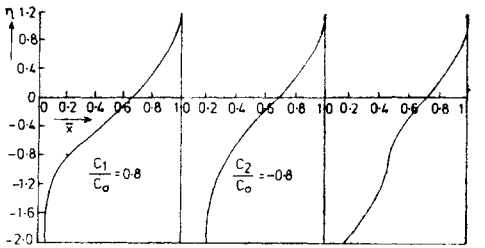

FIG. 11. Longitudinal velocity distribution in a non-shallow cavity for different values of $\frac{c_1}{c_0}$ and $\frac{c_2}{c_0}$.

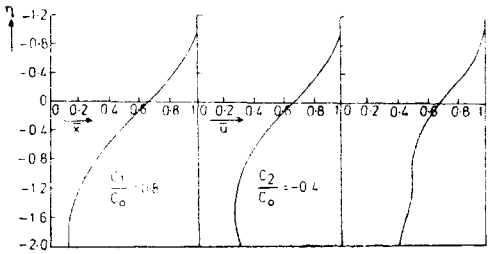

FIG. 12. Longitudinal velocity distribution in a non-shallow cavity for different values of $\frac{c_1}{c_0}$ and $\frac{c_2}{c_0}$.

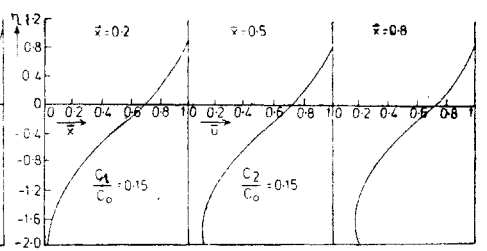

FIG. 13. Longitudinal velocity distribution in a non-shallow cavity for different values of $\frac{c_1}{c_0}$ and $\frac{c_2}{c_0}$.

Here $\bar{U}_1 = 0$ at $\bar{x} = 0$ and $\bar{x} = 1$ and the maximum velocity is reached at $\bar{x} = 0.5$ and its value is given by $(\bar{U}_1)_{max} = \frac{1}{6}$.

Profiles given in Fig. 11.

Case III : $\frac{c_1}{c_0} = 0.8, \frac{c_2}{c_0} = -0.4$.

Here $\bar{U}_1$ increases continuously from zero value to a maximum value at $\bar{x} = 1$.

$(\bar{U}_1)_{max} = 0.4$.

Profiles given in Fig. 12.

Case IV : $\frac{c_1}{c_0} = 0.15, \frac{c_2}{c_0} = 0.15$.

$\bar{U}_1$ increases continuously from zero to the maximum value 0.3 at $\bar{x} = 1$

Profiles given in Fig. 13.

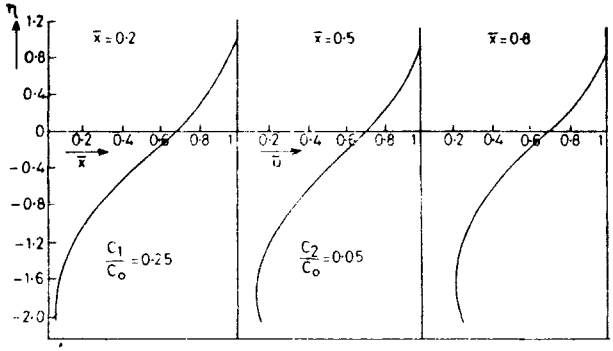

FIG. 14. Longitudinal velocity distribution in a non-shallow cavity for different values of $\frac{c_1}{c_0}$ and $\frac{c_2}{c_0}$.

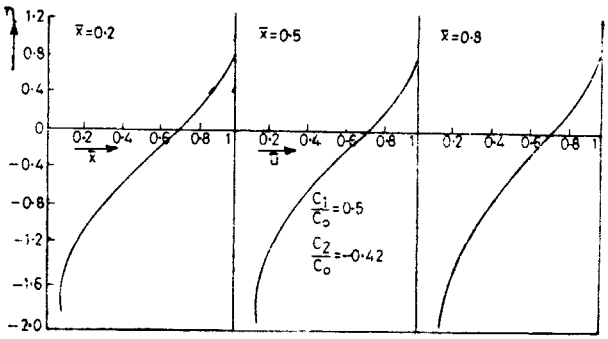

FIG. 15. Longitudinal velocity distribution in a non-shallow cavity for different values of $\frac{c_1}{c_0}$ and $\frac{c_2}{c_0}$.

Case V: $\frac{c_1}{c_0} = 0.25, \frac{c_2}{c_0} = 0.05$

$\overline{U}_1$ increases continuously from zero to the maximum value 0.3 at $\bar{x} = 1$. Profiles are given in Fig. 14.

Case VI: $\frac{c_1}{c_0} = 0.5, \frac{c_2}{c_0} = -0.42$.

$\overline{U}_1$ reaches a maximum value 0.15 at $\bar{x} = 0.6$ given in Fig. 15.

CONCLUSION

The theoretical velocity profiles in the turbulent mixing zone have been obtained assuming different distributions of velocity at the lower edge of the mixing zone, and a steady uniform flow above. Comparison with the experimental results for the shallow cavity ($L/D \approx 5$) where there is a strong reverse flow at the lower edge is

quite satisfactory. Experimental velocity distributions available when there is a co-flow in the cavity are rather approximate at the lower edge of the mixing zone and it is difficult to determine how the velocity varies along the length of the cavity. So comparison is difficult. But the peculiar nature of the velocity profiles for the cases (iv) and (v) where the velocity decreases reaches a minimum and then increases as η varies from 0.981 to —2.04 has not been observed in any of the experimental results. Probably the velocity distribution assumed at the lower edge for this case is different from experimental velocity distribution. To compare the results obtained with experimental results more accurate measurements of velocity distribution and velocity profiles are needed.

References

Charwat, A. P., Roos, J. N., Dwey, F. C., and Hitz, A. A. (1961). An investigation of separated flows Part I: The pressure field. *J. Aerospace Sci.*, **28**, p. 457–70.

——— (1961b). An investigation of separated flows Part II: Flow in the cavity and heat transfer. *J. Aerospace Sci.*, **28**, 513–27.

Fox, J. (1965). Flow regimes in transverse rectangular cavities. *Proceedings of the 1965 Heat Transfer and Fluid Mechanics Institute*, p. 230.

——— (1965 b). Heat transfer and air flow in a transverse rectangular notch. *Intern. J. Heat Mass Transfer*, 8, 269.

Haugen, R. L., and Dhanak, A. M. (1966). Momentum transfer in turbulent separated flow past a rectangular cavity. *J. appl. Mech.*, **33**, 641.

——— (1967). Heat transfer in turbulent boundary layer separation over a surface cavity. *J. Heat Transfer*, **89**, p. 335.

Kistler, A. L., and Tan, P. C. (1967). Some properties of turbulent separated flows. *The Physics of fluid snpplements*.

Majumdar, A. K., Debnath, K. D., and Ghosh, A. (1972). Flow in a shallow rectangular cavity. *Indian J. Tech.*, **10**, 6–10.

Maull, D. J., and East, L. P. (1963). Three dimensional flow in cavities. *J. Fluid Mech.*, **16**, 620–32.

Seban, R. A. (1965). Heat transfer and flow in a shallow rectangular cavity with subsonic turbulent air flow. *J. Heat Mass Transfer*, 3.

Seban, R. A., and Fox, J. (1961). Heat transfer to the air flow in a surface cavity. *Intern, Develop. Heat Transfer, A. S. M. E.*, p. 426.